

# Accuracy of the Post-Newtonian Approximation: Optimal Asymptotic Expansion for Quasi-Circular, Extreme-Mass Ratio Inspirals

Nicolás Yunes<sup>1</sup> and Emanuele Berti<sup>2</sup>

<sup>1</sup>*Institute for Gravitational Physics and Geometry and Center for Gravitational Wave Physics,  
Physics Department, The Pennsylvania State University, University Park, PA 16802, USA*

<sup>2</sup>*Jet Propulsion Laboratory, California Institute of Technology, Pasadena, CA 91109, USA*

(Dated: October 29, 2018)

We study the accuracy of the post-Newtonian (PN) approximation and its formal region of validity, by investigating its *optimal asymptotic expansion* for the quasi-circular, adiabatic inspiral of a point particle into a Schwarzschild black hole. By comparing the PN expansion of the energy flux to numerical calculations in the perturbative Teukolsky formalism, we show that (i) the inclusion of higher multipoles is necessary to establish the accuracy of high-order PN terms, and (ii) the region of validity of PN theory is largest at relative  $\mathcal{O}(1/c^6)$  (3PN order). The latter result suggests that the series diverges beyond 3PN order, at least in the extreme mass-ratio limit, probably due to the appearance of logarithmic terms in the energy flux. The study presented here is a first formal attempt to determine the region of validity of the PN approximation using asymptotic analysis. Therefore, it should serve as a template to perform similar studies on other systems, such as comparable-mass quasi-circular inspirals computed by high-accuracy numerical relativistic simulations.

PACS numbers: 04.25.Nx, 04.25.dg, 04.30.Db, 95.30.Sf

## I. INTRODUCTION

Before recent breakthroughs in numerical relativity (see e. g. [1] for a review), the post-Newtonian (PN) expansion had long been regarded as the best tool to predict the evolution of compact binaries. In spite of these great numerical advances, the PN approximation is still essential for the early inspiral phase, and especially for generic systems with arbitrary spins and eccentricities. Therefore, this approximation is still indispensable in the construction of templates for gravitational-wave detection through Earth- and space-based interferometers.

An accurate knowledge of the gravitational-wave phase is crucial for interferometric detection of compact binaries. In turn, the phasing accuracy crucially depends on the convergence (or divergence) properties of the PN expansion [2]. For this reason, the structure of the PN approximation has been extensively studied with the following two goals: to determine the region of validity of the series; and to improve its accuracy through resummation techniques. We shall not discuss the latter problem here, but we refer the reader to [3–10].

Early studies of the accuracy of the PN approximation focused on head-on collisions and on the quasi-circular inspiral of extreme-mass ratio (EMR) compact binaries. Simone *et al.* [11, 12] compared the relative  $\mathcal{O}(1/c^4)$ -accurate expansion of the energy flux to numerical perturbative calculations. They found that the series converges slowly for particles falling radially into black holes, remaining accurate for  $v/c \lesssim 0.3$ , where  $v$  is the orbital velocity and  $c$  is the speed of light. Building on previous work [13–16], Poisson [17] compared the energy flux for quasi-circular EMR inspirals computed with an  $\mathcal{O}(1/c^{11})$ -accurate PN expansion of black hole perturbation equations to numerical results. Poisson found that the PN series performs poorly for  $v/c \gtrsim 0.2$ , and that

higher-order terms do not necessarily increase the detection performance of the series, as measured by the fitting-factor with numerical waveforms. Various authors argued that the PN series should converge much faster for comparable-mass binaries (see e. g. [12, 18, 19]).

Previous studies of the accuracy of the PN expansion have been necessarily limited by the lack of accurate (ideally exact) numerical solutions of the non-linear Einstein equations, especially for the comparable-mass case. As increasingly accurate numerical evolutions of compact binaries become available, such convergence studies should be revisited, taking into account the improved knowledge of the “true” numerical evolution of the system. Until now, however, a systematic asymptotic analysis of the accuracy of the PN series was lacking. The term “asymptotic analysis” does not here refer to the study of the structure of the series at future or past null infinity. Instead, we mean those techniques applicable to *asymptotic series*, which arise as approximate solutions to non-linear partial differential equations.

In this paper, we perform an asymptotic analysis of the accuracy of the PN approximation by investigating the quasi-circular inspiral of EMR compact binaries. Asymptotic methods assume nothing about the convergence of the series, but only that it derives from the approximate solution to a *consistent* system of differential equations (see e. g. [20] for an introduction). In particular, we shall here search for the *optimal asymptotic expansion* of the PN series, i. e. for the truncation order beyond which the error in the series becomes larger than expected (that is, larger than the next term in the series). The main goal of this paper is to determine the approximate region of validity of the PN approximation for for quasi-circular EMR systems as a function of PN order.

The approximate region of validity is bounded by the region where the true error in the PN series is compara-

ble to the PN error estimate. By “true error” we here mean the difference between the PN estimate and the “exact solution” (i. e. the numerical result), while the “PN error estimate” is simply the next order term in the series. The orbital velocity will serve as the independent variable that labels this region, since this is a coordinate-invariant quantity, which for EMR systems is related to the angular velocity via  $\omega = v^3/M$ , with  $M$  the total mass of the system. The orbital velocity beyond which these two errors become comparable marks the region outside which one cannot neglect higher-order terms in the PN expansion. This is simply because, for larger velocities, the next order terms in the series are as large as the true error in the approximation.

Such an analysis requires we study the temporal evolution of the approximate solution to the Einstein equations. This could be achieved by investigating the PN expansion of several different quantities, such as the energy flux or the metric perturbation. The specific choice of PN-expanded quantity should not strongly affect the region of validity estimates, since all such quantities are expanded consistently to the same order. Here we choose to work with the energy flux, which is also an observable and a coordinate-invariant quantity.

The consistency of this analysis hinges, of course, on the error contained in the “exact” numerical solution. For the asymptotic analysis to succeed, this numerical error must be smaller than the PN error estimate. For example, if we investigate the region of validity of some PN quantity to relative  $\mathcal{O}(1/c^4)$ , the numerical error must be smaller than the terms of relative  $\mathcal{O}(1/c^5)$  in the series. The energy flux of EMR systems can be accurately modeled through the Teukolsky perturbative formalism, which, coupled to Green-function methods and spectral integrators, guarantees here a numerical accuracy of  $\mathcal{O}(10^{-6})$ . We shall see that this numerical accuracy suffices to perform an asymptotic analysis of the PN series to relative  $\mathcal{O}(1/c^{11})$  in the most interesting range of the particle’s orbital velocity.

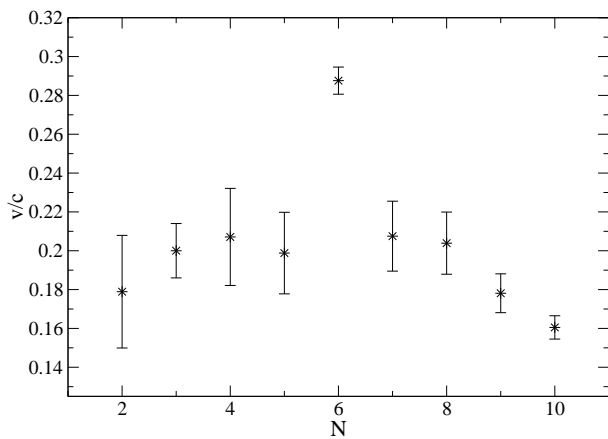


FIG. 1: Edge of the region of validity for different PN orders.

The edge of the region of validity of the PN series for

quasi-circular EMR compact binaries as a function of PN order  $N$  is given by Fig. 1. These results verify and extend those of Simone, *et al.* [11, 12]. The error bars in this figure symbolize the uncertainty inherent in the definition of the edge of the region of validity of any asymptotic series, which is defined more accurately in Sec. II below. For relative  $\mathcal{O}(1/c^6)$  and smaller the PN solution seems to have a “convergent” character, since the region of validity either increases or remains roughly constant with PN order. On the other hand, for larger than relative  $\mathcal{O}(1/c^6)$  there is a “divergent” behavior, reflected in the shrinking of the region of validity with increasing PN order. As we shall see, this may be associated with the appearance of logarithms at high orders in the PN approximation. Similar conclusions were reached by Porter [8–10], when studying how to increase the accuracy of the PN series through Chebyshev resummation.

A by-product of this analysis is the determination of the *minimum* number of multipoles needed in the numerical energy flux to perform *any* type of comparison with the PN approximation as a function of velocity. These results are presented in Table I, which provides an easy reference to determine how many multipoles are needed to have an accuracy comparable to the  $\mathcal{O}(1/c^N)$  PN approximation. For example, if one requires an accuracy of relative  $\mathcal{O}(1/c^6)$ , then one need only include up to  $\ell = 2$  between  $0.298 < v/c < 0.408$ , up to  $\ell = 3$  between  $0.131 < v/c < 0.298$  and up to  $\ell = 4$  for  $v/c < 0.131$ . Remarkably, for large velocities one can usually simply look at the  $\ell = 2$  multipole, while for small velocities one must include more and more multipoles. Such a result is a consequence of individual multipolar contributions being fairly velocity-independent in the large velocity regime.

The analysis presented in this paper provides a general, gauge-independent and systematic method to study the region of validity of the PN approximation for any system. We concentrate on EMR binaries here for simplicity, but the method can be straightforwardly extended to comparable-mass, spinning or eccentric binaries. This method is more systematic and general than that of Simone, *et al.* [12], and it is similar in spirit to the “PN diagnostic” scheme [19, 21–23]. In this scheme, however, comparisons with numerical simulations are carried out considering time-independent, conserved quantities in a quasi-equilibrium framework. We hope that the analysis presented here provides a template for numerical relativity groups to test the convergence (or divergence) of the PN approximation, which is of great interest both to the PN and data analysis communities.

The remaining of this paper presents more details of our methods and results, and it is organized as follows. Section II summarizes the basics of asymptotic analysis, formally defining optimal asymptotic expansions and providing a pedagogical example of how to determine the region of validity of an asymptotic series. Section III reviews the energy flux of EMR compact binaries in quasi-circular orbits as obtained in perturbation theory and PN theory. Section IV calculates the region of validity of the

PN approximation through asymptotic techniques. Section V concentrates on the number of multipoles needed

in the numerical energy flux to test PN theory. Section VI concludes and points to future research.

$\ell_{\min}$	$N = 2$	$N = 3$	$N = 4$	$N = 5$	$N = 6$	$N = 7$	$N = 8$	$N = 9$	$N = 10$	$N = 11$
2	0.408	0.408	-	0.408	0.408	0.408	-	0.408	-	-
3	-	0.101	0.408	0.298	0.306	0.402	0.408	0.379	0.408	-
4	-	-	-	0.057	0.131	0.251	0.303	0.275	0.322	0.408
5	-	-	-	-	-	0.039	0.123	0.144	0.212	0.349
6	-	-	-	-	-	-	-	-	0.067	0.247

TABLE I: Minimum velocity at which we need to include a minimum of  $\ell_{\min}$  multipoles to get an accuracy corresponding to the  $N$ th PN term.

In this work we follow the conventions of Misner, Thorne and Wheeler [24]: the metric has signature  $(-, +, +, +)$ , and unless otherwise specified we use *geometrical units* where  $G = c = 1$ . The notation  $\mathcal{O}(A)$  stands for terms of relative order  $A$ , where  $A$  is dimensionless. Therefore, PN remainders are denoted as  $\mathcal{O}(v/c)^q = \mathcal{O}(1/c^q) = \mathcal{O}(v^q)$ , where  $q$  is an integer. When we say a quantity is of  $p$ th PN order we mean that it is accurate to relative  $\mathcal{O}(1/c^{2p})$ . The standard asymptotic notation will also be used extensively in this paper, and it is defined in the next section.

## II. ASYMPTOTIC SERIES

In this section we shall review the basic properties of asymptotic series. We refer the reader to [20, 25] for more details. We begin by defining remainders and asymptotic series, and continue with a description of their convergent and divergent properties. We then define the concept of an optimal asymptotic expansion, using which we can estimate the region of validity of an asymptotic series. We conclude this section with a pedagogical example of such a calculation applied to Bessel functions.

### A. Basic definitions and notation

Consider some partial or ordinary, linear or non-linear differential equation, whose solution is  $f(x)$ . Consider also a partial sum of the form

$$s_N(x) = \sum_{n=0}^N a_n (x - x_0)^n. \quad (1)$$

We here choose such a partial sum for simplicity, but in general there could be a controlling factor, such as an exponential function, that multiplies the partial sum.

Let us then define the remainder  $\epsilon_{(N)}(x)$  as

$$\epsilon_{(N)}(x) \equiv f(x) - s_N(x). \quad (2)$$

The limit as  $N \rightarrow \infty$  of the partial sum,  $s_\infty(x)$ , is said to be *asymptotic to* the function  $f(x)$  as  $x \rightarrow x_0$ , i. e.  $f(x) \sim s_\infty(x)$  as  $(x \rightarrow x_0)$ , if and only if

$$\epsilon_{(N)}(x) \ll (x - x_0)^N, \quad (x \rightarrow x_0), \quad (3)$$

for all  $N$ . The symbol  $\sim$  here is used exclusively to mean “asymptotic to” and is never intended to mean “approximately,” which shall be denoted via the symbol  $\approx$ . Similarly, the symbol  $\ll$  has a specific definition: if  $f(x) \ll g(x)$  as  $x \rightarrow x_0$ , then

$$\lim_{x \rightarrow x_0} \frac{f(x)}{g(x)} = 0. \quad (4)$$

Then,  $f(x) \sim s_\infty(x)$  as  $x \rightarrow x_0$  if and only if

$$\lim_{x \rightarrow x_0} \frac{f(x)}{s_N(x)} = 1. \quad (5)$$

There are more formal definitions of an asymptotic series, but this one will suffice for the analysis of this paper. From this definition, it follows that all Taylor series are asymptotic series as well.

Such a definition of an asymptotic series has a clear physical meaning: a power series is asymptotic to some function if the remainder after  $N$  terms is much smaller than the last retained term as  $x \rightarrow x_0$ . In this sense, the PN expansion of any quantity is an asymptotic series to the exact solution of the Einstein equations as  $v \rightarrow 0$ . This is so because one expects there to exist a velocity region where the remainder of the PN expansion after  $N$  terms is much smaller than the last retained term in the series. Such a remainder, of course, can only be computed once an exact or numerical solution is known.

## B. Convergent and divergent series

An important consequence of the above definition is that asymptotic series need not be convergent. A series is convergent if and only if

$$\lim_{N \rightarrow \infty} \epsilon_{(N)} = 0, \quad (6)$$

for all  $x$  inside a given radius of convergence  $R$  around  $x_0$ , i. e. for  $|x - x_0| < R$ . The radius of convergence can be computed via the standard Cauchy ratio test:

$$R = \lim_{n \rightarrow \infty} \frac{a_n}{a_{n+1}}, \quad (7)$$

where  $a_n$  is the  $n$ th term in the series.

The convergence requirement of Eq. (6) is much stronger than the asymptotic requirement of Eq. (3). The main difference is that in the asymptotic definition the remainder need not go to zero as  $N \rightarrow \infty$ . Thus, asymptotic series can be divergent. In fact, such series often approach the exact or numerical solution much faster than any convergent series. However, if one insists on adding higher-order terms to the series for some fixed value of  $x$  (or if one pushes the approximation to  $x \gg x_0$ ), eventually the series will diverge. Thus, a correct use of asymptotic series forces us to truncate them before the answer deviates too much from the exact solution.

The concept of convergence is said to be *absolute*, because it is an intrinsic property of the coefficients  $a_n$  and it requires no knowledge of the exact solution  $f(x)$ . On the other hand, the concept of asymptoticity is said to be *relative* because it requires knowledge both of the coefficients and of the exact or numerical solution. This is the reason why analyses of the asymptoticity of the PN series were not possible before the recent numerical relativity breakthroughs.

## C. Optimal asymptotic expansion

Suppose that we only know a limited number of terms in a (possibly divergent) series. We want to determine the optimal number to include in the partial sum to get an answer as close as possible to the exact solution, i. e. the so-called *optimal asymptotic expansion*. In asymptotic language, we are looking for the partial sum that minimizes the remainder in the approximation.

More precisely, the procedure is as follows: (i) Choose some fixed value of  $|x - x_0|$ , so that the series becomes a sum of  $N$  numerical coefficients. In PN theory, these coefficients will in general be functions of the symmetric mass ratio  $\eta \equiv m_1 m_2 / (m_1 + m_2)^2$ , of the spins of the binary members and of the eccentricity parameters; (ii) For this fixed  $|x - x_0|$ , search over the individual coefficients in the series. Typically these terms initially decrease in magnitude, but eventually diverge; (iii) Let the first minimum in the sequence occur when  $n = M$  such

that  $M < N$ ; (iv) The partial sum of all terms in the series up to (but not including) the  $M$ th term is the optimal asymptotic expansion. The  $M$ th term is also an approximate measure of the error in the optimal asymptotic expansion, because it is asymptotic to the  $M$ th remainder as  $x \rightarrow x_0$ . Thus, the optimal asymptotic expansion minimizes the remainder, since if we kept on adding more terms the remainder would diverge.

This method works nicely when we have a large number of terms in the series. Unfortunately, it does not work very well in PN theory, where usually only a few terms are known. Moreover, this method depends on the chosen value of  $|x - x_0|$ . In PN theory, it is precisely this value of  $|x - x_0|$  that we wish to determine. Nonetheless, we can adapt the method to find the region of validity of any PN series, as we show below.

## D. Region of validity

Let us invert the premise and look for the *region of validity* as a function of the number of terms kept in the series. This region can be defined as the region inside which the remainder  $\epsilon_{(N)}$  and the  $(N + 1)$ th term in the series are of the same order. If the series is asymptotic to the exact solution, we then expect  $s_N$  to be the best approximation to  $f(x)$  for all  $x \leq \bar{x}$  with

$$\mathcal{O} [\epsilon_{(N)}(\bar{x})] = \mathcal{O} (\bar{x} - x_0)^{N+1}. \quad (8)$$

The convergent or divergent character of the asymptotic series determines how  $\bar{x}$  behaves as a function of the number of terms kept in the series. If the series is convergent, like a Taylor expansion, then we expect the accuracy of the series to increase as more terms are added. This is so provided  $\bar{x}$  is inside the radius of convergence, but as already discussed, this is always the case because Eq. (6) is stronger than Eq. (3). Therefore, it follows that  $\bar{x}$  tends to increase, and in fact approach the radius of convergence, as the number of terms kept in the series increases. On the other hand, if the series is divergent, then the opposite is true, namely as more terms are kept in the series,  $\bar{x}$  decreases. This is so because higher-order terms tend to diverge faster than lower-order ones.

The order symbol encodes here a certain arbitrariness rooted in asymptotic analysis. In other words, one must decide a priori how different the right and left-hand side of Eq. (8) should be before equality is declared. This ambiguity means that there is not a precise value for the region of validity of an asymptotic approximation. Instead, this concept is ambiguous up to the order symbol. In spite of this ambiguity, we can still arrive at important qualitative conclusions through such an analysis, provided we quantify the ambiguity with error bars, as done in later sections.

### E. A pedagogical example: The modified Bessel function

Before turning to an analysis of the PN series, in this section we shall clarify the definitions of previous sections with a relatively simple pedagogical example. Consider then the following differential equation

$$x^2 \frac{d^2 y}{dx^2} + x \frac{dy}{dx} - (x^2 + 25) y = 0, \quad (9)$$

$$I_5^{(12)} = \frac{e^x}{\sqrt{2\pi x}} \left[ 1 - \frac{99}{8} \frac{1}{x} + \frac{9009}{128} \frac{1}{x^2} - \frac{225225}{1024} \frac{1}{x^3} + \frac{11486475}{32768} \frac{1}{x^4} - \frac{43648605}{262144} \frac{1}{x^5} - \frac{305540235}{4194304} \frac{1}{x^6} - \frac{3011753745}{33554432} \frac{1}{x^7} \right. \\ - \frac{376469218125}{2147483648} \frac{1}{x^8} - \frac{7905853580625}{17179869184} \frac{1}{x^9} - \frac{412685556908625}{274877906944} \frac{1}{x^{10}} - \frac{12793252264167375}{2199023255552} \frac{1}{x^{11}} \\ \left. - \frac{1829435073775934625}{70368744177664} \frac{1}{x^{12}} + \mathcal{O}(1/x)^{13} \right]. \quad (10)$$

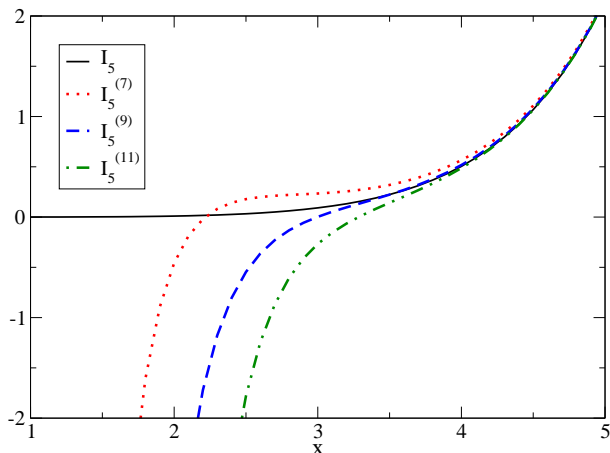


FIG. 2: Plot of the modified Bessel function (solid) and its asymptotic expansion of order  $N = 7$  (dotted),  $N = 9$  (dashed) and  $N = 11$  (dot-dot-dashed).

Figure 2 shows the exact numerical solution to the modified Bessel function (solid) and its  $N = 7$  (dotted),  $N = 9$  (dashed) and  $N = 11$  (dot-dot-dashed) asymptotic expansions. The figure clearly shows two important features of this asymptotic series: (i) The series can be extremely accurate quite far from its singular point of expansion  $x = \infty$ . In principle, there is no *a priori* reason to believe that any of these approximations will be accurate in the domain plotted, since  $x = 5$  is far from  $x = \infty$ . Nonetheless, all expansions plotted are quite close to the numerical answer, even up to  $x \approx 3$ ; (ii) The higher the order  $N$  of the asymptotic expansion, the smaller its region of validity. Observe that the  $N = 11$  ( $N = 7$ ) expansion roughly deviates from the numerical answer when  $x \approx 3$  ( $x \approx 2$ ). As already discussed, this behavior is usually associated with divergent asymptotic

One recognizes Eq. (9) as the modified Bessel equation with index  $\nu = 5$  (see e. g. [26]). The modified Bessel equation does not have a known closed-form solution valid everywhere in its domain, and the numerical solution of this equation is called a modified Bessel function:  $y(x) = I_5(x)$ . The asymptotic expansion of the modified Bessel function as  $x \rightarrow \infty$ , say  $I_5^{(N)}$ , can be found at any given order  $N$ . For  $N = 12$ , for example, we have:

series near the edge of their region of validity.

As a check of this statement, let us now determine the region of validity of this asymptotic expansion. As explained earlier, this region will depend on  $N$ , the order of the asymptotic expansion. From Eq. (2) we see that the remainder is given by  $\epsilon_{(N)} = I_5 - I_5^{(N)}$ . Noting that the  $N$ th order term in the asymptotic series is simply  $I_5^{(N)} - I_5^{(N-1)}$ , the region of validity is defined by the relation [Eq. (8)]

$$\mathcal{O}(I_5 - I_5^{(N)}) = \mathcal{O}(I_5^{(N+1)} - I_5^{(N)}). \quad (11)$$

Here it suffices to search for the intersection between these two curves.

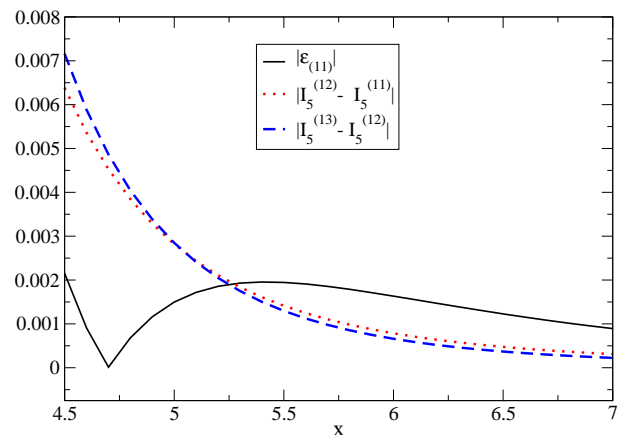


FIG. 3: Plot of the absolute value of the remainder of the  $N = 11$  asymptotic expansion of the modified Bessel function (solid), the  $N = 12$  term (dotted) and the  $N = 13$  term (dashed). The kink in the solid line is due to the use of the absolute value operator.

$n$	$\bar{x}$	$\delta\bar{x}$	$\delta I_5^{(N)}$ [%]
11	5.27	0.22	0.06
10	4.70	0.26	0.34
9	4.11	0.03	2.16
8	3.51	0.04	17.7

TABLE II: Approximate edge of the region of validity ( $x = \bar{x}$ ) for different asymptotic expansions of the modified Bessel function. We also present an approximate measure of the error in  $\bar{x}$ , as well as the fractional relative error in  $I_5^{(N)}$ , that is  $\delta I_5^{(N)} = 100(I_5 - I_5^{(N)})/I_5$ , evaluated at  $\bar{x}$ .

Figure 3 plots the absolute value of the remainder of the  $N = 11$  expansion (solid), the  $N = 12$  term (dotted) and the  $N = 13$  term (dashed). For  $x \gtrsim 5.25$  the exact error in the  $N = 11$  expansion relative to the numerical answer is larger than the terms neglected in the approximation, while for  $x \lesssim 5.25$  the opposite is true. Therefore, the intersection of the solid and dotted curves defines *approximately* the edge of the region of validity for the  $N = 11$  partial sum:  $\bar{x} \approx 5.25$ .

This analysis can be repeated for any  $N$  and the results are presented in Table II, which reproduces and extends results in Table 3.1 of [20]. The error bars presented in the third column are given by the difference between  $\bar{x}$  and the intersection of the  $(N + 2)$ -term with  $N$ th-order remainder. They serve as a reminder that all quantities are asymptotic in nature, and thus, can only be interpreted in an *approximate* sense.

Table II presents several features that are of interest. First, observe that the region of validity decreases as the order of the expansion increases (the region of validity is  $\{\bar{x}, \infty\}$ , so if  $\bar{x}$  increases, the region of validity decreases). As explained earlier, this is an important feature of divergent asymptotic expansions, due to higher-order terms diverging sooner than lower-order ones as we approach the edge of the region of validity. Second, observe that higher-order partial sums are much more accurate than low-order ones, when evaluated at their respective edges of validity. For example, the  $N = 11$  expansion has an error of only 0.06% relative to the exact numerical answer when evaluated at  $x \approx 5.3$ . This is a sensible feature of optimal asymptotic expansions, i. e. higher-order approximations should be more accurate than lower-order ones.

The region of validity of an asymptotic expansion should be interpreted with caution. In fact, the asymptotic expansion of the Bessel function could be used outside its region of validity, as defined here. The risk of using the  $N$ th-order approximation beyond  $\bar{x} - \delta\bar{x}$  is that of making errors *larger* than those supposedly contained in the approximation. For example, the  $N = 11$  expansion of the Bessel function produces a fractional error of (0.2, 3.5, 36.5)% relative to the numerical answer when evaluated at  $x = (4.5, 4.0, 3.5)$ , which is always larger than the next-order term in the approximation. There-

fore, beyond the region of validity as defined here, neglecting the next order term in the approximation leads to larger and larger errors relative to the exact numerical solution.

### III. EXTREME-MASS RATIO INSPIRALS

In this section we shall apply the previously-discussed asymptotic tools to the inspiral of a small compact object around a supermassive black hole (an EMR system). We shall thus consider a black hole of mass  $m_1 = M$  and a much smaller object of mass  $m_2 = \mu \ll M$ . We shall further focus on the adiabatic quasicircular inspiral phase, where the radiation-reaction timescale is much larger than the orbital period.

Such a system is an excellent testbed for the methods discussed above. The PN approximation of several quantities is known to very high order in the EMR limit. Furthermore, we can numerically compute the energy flux with perturbative techniques that are very accurate for all velocities.

Before turning to the study of the region of validity of the PN approximation, in the following sections we briefly review the derivation and accuracy of the numerical solution in black hole perturbation theory and the analytical structure of the PN expansion of the flux. We also present a simple graphical comparison of the PN results with the numerical solution.

#### A. Numerical calculation of the energy flux

An exact solution is necessary if we want to use asymptotic analysis to determine the region of validity of the PN approximation in the extreme mass-ratio limit (henceforth denoted PN-EMR approximation). This “exact” solution can be found numerically through the use of black hole perturbation theory. Let us then express the metric as a background (in our case, the Schwarzschild metric) plus a perturbation:

$$g_{\alpha\beta} = g_{\alpha\beta}^{(0)} + h_{\alpha\beta}, \quad (12)$$

with the perturbation assumed to be small, i. e.  $|h_{\alpha\beta}| \ll |g_{\alpha\beta}^{(0)}|$ . The Einstein equations are then linearized in  $h_{\alpha\beta}$  and rewritten in terms of the perturbed Weyl Scalar  $\delta\Psi_4(t, r, \theta, \phi)$ . In turn, the perturbed Weyl scalar can be decomposed into multipolar components. Working in the frequency domain and using spin-weighted spherical harmonics  ${}_{-2}Y_{\ell m}(\theta, \phi)$ , these components are

$$\Psi_{\ell m}(\omega, r) = \frac{1}{2\pi} \int d\Omega dt e^{i\omega t} {}_{-2}Y_{\ell m}^*(\theta, \phi) [r^4 \delta\Psi_4(t, r, \theta, \phi)], \quad (13)$$

The coefficients of the harmonic decomposition obey an inhomogeneous differential equation, the Bardeen-Press-Teukolsky equation, where the source term is the harmonic decomposition of the stress-energy tensor of the

orbiting particle. Due to the symmetries of the source term, the multipolar components satisfy the symmetry relation

$$\Psi_{\ell m}^*(r, \omega) = (-1)^\ell \Psi_{\ell -m}^*(r, -\omega). \quad (14)$$

The Bardeen-Press-Teukolsky equation can be solved in the adiabatic approximation with Green-function methods in the frequency-domain [27, 28]. Our numerical code has been described in detail in [29–32].

The perturbed Weyl scalar can be used to reconstruct the fluxes of energy and momentum at infinity. This is so because these fluxes are related to  $h_{\alpha\beta}$  at infinity, which can be computed from convolution integrals of  $\Psi_{\ell m}(\omega, r)$  and the (Fourier-decomposed) spherical-harmonic components of the stress-energy tensor. For circular orbits, the multipolar components of the energy flux  $F_{\ell m} \equiv \dot{E}_{\ell m}$  (where  $|m| \leq \ell$ ) satisfy the symmetry property

$$F_{\ell -m} = F_{\ell m}, \quad (15)$$

so we can limit consideration to multipoles with  $m > 0$ . Therefore, when we refer to “the relative contribution of the  $(\ell, m)$  multipole to the total flux” we are really considering *twice*  $F_{\ell m}$ . The angular momentum flux is related to the energy flux through the particle’s orbital frequency  $\Omega$ , related to the orbital velocity via  $v = (M\omega)^{1/3}$ . We have computed the energy flux including multipoles up to  $\ell_{\max} = 8$  for a thousand equispaced velocities in the range  $v \in [10^{-2}, v_{\text{ISCO}}]$ , where the orbital velocity at the ISCO  $v_{\text{ISCO}} = 6^{-1/2} \simeq 0.408$ .

The Teukolsky formalism has inherent errors, but it possesses some distinct advantages over the PN expansion. The principal advantage is that no restriction on the velocities is necessary: the numerical solution is valid to all orders in  $v$ . For this reason the numerical solution is not only compatible with the PN-EMR approach, but it is also very convenient to study the latter’s region of validity. Formally speaking, the PN-EMR approximation is a bivariate expansion in two independent parameters:  $v \ll 1$ , such that the gravitational field is weak and all bodies move slowly (PN approximation); and  $\mu/M \ll 1$ , that enforces the EMR limit. Therefore, there are two independent uncontrolled remainders of relative  $\mathcal{O}(N, M)$ , which stands for errors of relative  $\mathcal{O}(1/c)^N$  and  $\mathcal{O}(\mu/M)^M$ . The perturbative approach is valid to relative  $\mathcal{O}(\infty, 0)$ , whereas the PN-EMR expansion (discussed below) is only available up to relative  $\mathcal{O}(11, 0)$ .

The asymptotic tools discussed in this paper hinge on controlling the numerical error inherent in the “exact” solution. These errors cannot always be modeled analytically (see [27, 28] for a detailed discussion). When we consider the energy flux for a circular, adiabatic inspiral, the dominant errors can be roughly divided in two groups:

- (1) **Truncation errors**, due to neglecting high- $\ell$  multipoles in the multipolar decomposition of  $F_{\ell m}$ ;
- (2) **Discretization errors**, due to solving numerically the inhomogeneous Teukolsky equation.

Truncation errors tend to increase with orbital velocity, and to a certain extent they can be modeled analytically. Poisson [13] has shown that, for a given  $\ell$ , the luminosity is dominated by modes with even  $\ell + m$ , while the power radiated by modes with odd  $\ell + m$  is suppressed by roughly a factor  $v^2$ . Since the total power radiated in the  $\ell$ th multipole scales like

$$F_\ell \propto v^{(2\ell-4)}, \quad (16)$$

the error on the flux due to truncating at some  $\ell = \ell_0$  can be approximated by  $\delta F_{\ell_0} \approx v^{2\ell_0-2}$ . Equation (16) provides a simple rule of thumb to determine the number of multipoles required to achieve a given fractional truncation accuracy  $\epsilon_{(\ell)}$ : we must include multipolar components up to  $\ell_{\max}$ , where  $v^{(2\ell_{\max}-4)} \sim \epsilon_{(\ell)}$  [27]. According to this rule of thumb, including up to  $\ell_{\max} = 8$  (as we do, unless otherwise stated) yields a truncation accuracy *better* than  $\epsilon_{(\ell)} \approx 10^{-6}$  up to  $v \simeq 0.316$ , while at the ISCO we have an accuracy better than  $\epsilon_{(\ell)} \approx 2 \times 10^{-5}$ .

Discretization error is kept small by use of adaptive ordinary differential equation integrators to solve the Bardeen-Press-Teukolsky equation, and Gauss-Legendre spectral methods to compute convolution integrals [33]. We investigated this error by experimenting with tolerance parameters in the integrators and increasing the number of points in the spectral methods. We found that discretization error at low velocities is very sensitive to other details of the code, such as the accuracy in the numerical inversion yielding  $r(r_*)$ , where  $r$  is the Schwarzschild radius and  $r_*$  is the tortoise coordinate. At small velocities and large radii we obtain agreement with Ref. [28] to a six-digit level, so we estimate the discretization error to be roughly of  $\mathcal{O}(10^{-6})$  (and possibly smaller at larger velocities). This is confirmed by the low-velocity, low-amplitude region of Fig. 6 below, where oscillations due to discretization error appear only for  $v \lesssim 10^{-2}$ . These oscillations are in fact of  $\mathcal{O}(10^{-7})$  relative to the dominant Newtonian flux.

Before proceeding to the PN expansion of the energy flux in the EMR limit, we must mention that both the perturbative calculation and the PN expansion neglect absorption of radiation by the black hole. Poisson and Sasaki [14] have shown that this absorption is negligible with respect to the energy carried off to infinity, being suppressed by a factor of  $v^8$ . Although these terms might modify the energy flux ever so slightly, both the numerical and PN flux considered here consistently neglect them. Therefore, these terms cannot affect any conclusions regarding the region of validity of the PN approximation.

## B. PN expansion of the energy flux

The PN approximation is an expansion in small velocities  $v \ll 1$ , but to model EMR systems we also expand in  $\mu/M \ll 1$ . In this PN-EMR approximation the energy

flux is given by [16, 17]

$$F^{(N)} = F_{\text{Newt}} \left[ \sum_{k=0}^N (a_k + b_k \ln v) v^k \right], \quad (17)$$

where  $N$  labels the  $N$ th-order partial sum or PN approximant (known up to  $N = 11$  in the PN-EMR approximation),  $a_1 = b_1 = b_2 = b_3 = b_4 = b_5 = b_7 = 0$ , and the remaining coefficients can be found in Eq. (3.1) of Ref. [16]. As explained in the Appendix, the logarithms do not affect the applicability of asymptotic methods in the velocity regions of interest. Here  $v$  is the orbital velocity, and the Newtonian flux is given by

$$F_{\text{Newt}} = -\frac{32}{5} \mu^2 v^{10} M^2. \quad (18)$$

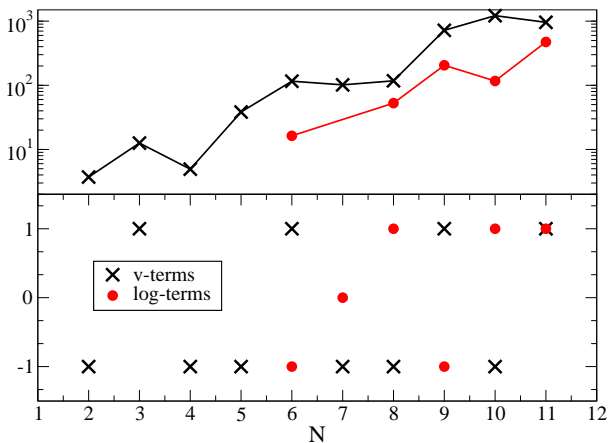


FIG. 4: Top panel: plot of the absolute magnitude of the coefficients of the flux as a function of PN order in a log-linear plot. Bottom panel: plot of the sign of the coefficients of the flux as a function of PN order. Crosses and circles denote polynomial ( $a_k$ ) and logarithmic ( $b_k$ ) terms, respectively.

The structure of the PN-EMR series is worth discussing further. The series is composed of two distinct types of terms: those that depend only on a certain power of the velocity, and those that include a logarithmic dependence. Since  $b_6 \neq 0$ , the logarithmic terms appear first at  $\mathcal{O}(1/c)^6$ . Furthermore, as shown graphically in Fig. 4, the sequence of coefficients  $a_k$  or  $b_k$  does not present a clear alternating pattern. Finally, the absolute magnitude of the coefficients in the series is not of order unity, as expected of a convergent series. Instead, their magnitude grows drastically with increasing order. Such a pathological behavior is not present in the comparable-mass limit of the PN expansion (see e. g. [18, 19] for a discussion).

### C. Comparison of PN-EMR and numerics

The energy flux computed both numerically and within the PN-EMR framework is plotted in Fig. 5 as a function of orbital velocity. Here and below, we shall present

error bars in all figures only when these errors are visible (e. g. if the  $y$ -axis scale is of  $\mathcal{O}(10^{-1})$ , the numerical error won't be presented, since error bars of  $\mathcal{O}(10^{-6})$  would not be visible). Figure 5 is very similar to Fig. 1 of [17], except that here the numerical result is computed including terms up to  $\ell_{\text{max}} = 8$  and we show all terms up to 5.5PN order in the flux.

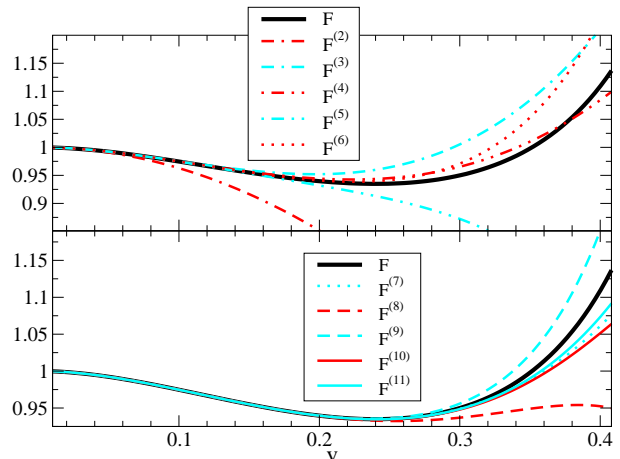


FIG. 5: Plot of the total energy flux  $F$  computed numerically (solid) and at different PN orders in the PN-EMR approximation. Odd orders are plotted in a lighter gray, while even orders are plotted in darker gray. Line styles are as follows:  $F^{(2)}$ ,  $F^{(3)}$  is dash-dash-dot;  $F^{(4)}$ ,  $F^{(5)}$  is dash-dot-dot;  $F^{(6)}$ ,  $F^{(7)}$  is dotted;  $F^{(8)}$ ,  $F^{(9)}$  is dashed;  $F^{(10)}$ ,  $F^{(11)}$  is solid. To avoid cluttering, the top panel shows  $F^{(2)}$  up to  $F^{(6)}$  and the bottom panel shows  $F^{(7)}$  up to  $F^{(11)}$ .

For low velocities ( $v \lesssim 0.2$ ) all PN approximants (except for the 1PN curve) agree well with the numerical result, while in the high-velocity region ( $v \gtrsim 0.2$ ) the lower-order PN approximants deviate from the numerical answer. Such a behavior is reminiscent of that first discussed by Poisson [17]. Typically, and roughly speaking, the partial sums seem to approach the numerical result as we increase the PN order. The question we shall answer in the next section is whether this approach occurs at the expected rate for the given order.

The accuracy of the PN approximants is better seen in Fig. 6, where we plot the moduli of the remainders  $|F^{(N)} - F|$ . Light and dark gray curves correspond to odd and even PN orders respectively. We plot here only the region  $v < 0.014$ , since for smaller velocities the remainders are smaller than  $\mathcal{O}(10^{-6})$ , and hence contaminated by numerical error. Observe that the dominant even-order remainders decrease monotonically with order until  $\epsilon_{(4)}$  and  $\epsilon_{(6)}$  cross at  $v \lesssim 0.257$  (dark gray square). Similarly, the dominant odd-order remainders also decrease monotonically until  $\epsilon_{(3)}$  and  $\epsilon_{(5)}$  cross at  $v \lesssim 0.265$  (light gray square). This behavior is “convergent” in nature, but the region of convergence seems to be larger when odd or even terms are considered separately. Such a result derives perhaps from the fact that even and odd terms are physically different, coming respectively from a



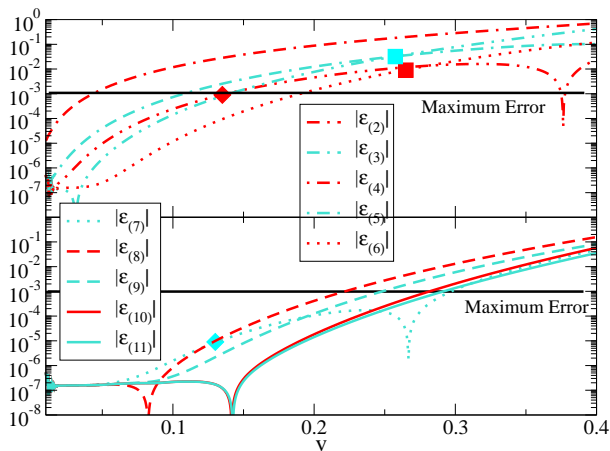


FIG. 6: Moduli of the remainders  $|F^{(N)} - F|$  as a function of velocity. Light gray curves correspond to odd PN orders, while dark gray curves correspond to even orders. Line styles are the same as in Fig. 5. The light gray (dark gray) squares mark the intersection of  $\epsilon_{(4)}$  and  $\epsilon_{(6)}$  ( $\epsilon_{(3)}$  and  $\epsilon_{(5)}$ ). The light gray (dark gray) diamonds mark the intersection of  $\epsilon_{(4)}$  and  $\epsilon_{(5)}$  ( $\epsilon_{(7)}$  and  $\epsilon_{(8)}$ ). Numerical discretization errors at low velocities are of order  $10^{-6}$  (see Section IIIA), therefore remainders smaller than about  $10^{-6}$  have no physical meaning.

sum over multipoles moments and integrals of these over the entire propagation history of the waves.

When all orders are considered simultaneously, the PN approximation still presents a convergent-like behavior, but in a reduced region. This reduction is due to the crossing of  $\epsilon_{(4)}$  and  $\epsilon_{(5)}$  at  $v \approx 0.135$  (dark gray diamond) and the crossing of  $\epsilon_{(7)}$  and  $\epsilon_{(8)}$  at  $v \approx 0.125$  (light gray diamond). Note also that the “region of convergence” should not be confused with the “region of validity.” By the former we mean the region where the  $(N+1)$ th-order remainder is smaller than the  $N$ th-order one. The latter is the region where the asymptotic expansion is valid (the remainder is of the same order as the next-order term), and it will be discussed in more detail by asymptotic techniques in section IV below.

In the large velocity region of Fig. 6, the convergent-like behavior is replaced by a divergent one. For example,  $\epsilon_{(4)}$  becomes more accurate than  $\epsilon_{(5)}$  for  $v > 0.135$ . Similarly,  $\epsilon_{(7)}$  seems more accurate than  $\epsilon_{(8)}$  for  $v > 0.125$  (see also Table III in the next section), and in fact  $\epsilon_{(7)}$  is strikingly accurate for  $0.2 < v < 0.35$ —much better than  $\epsilon_{(8)}$  and  $\epsilon_{(9)}$ . This suggests that the region of validity of lower-order approximations may be actually larger than that of higher-order ones. In other words, the region of validity seems to *shrink* with increasing order. Asymptotic techniques are ideal to study the edge of the region of validity for high-velocities.

The convergent/divergent transition is hard to see in Fig. 6, so for clarity Fig. 7 plots the remainder as a function of PN order  $N$  for four selected values of  $v$ . Until now, we have always included multipoles up to  $\ell = 8$ , but here we explore the multipolar dependence,

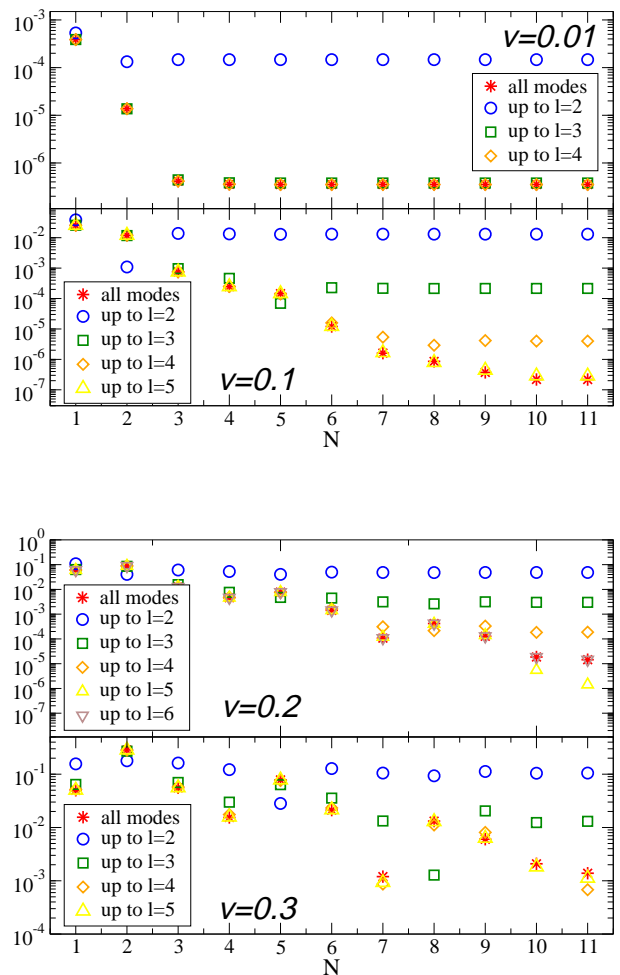


FIG. 7: Plot of the absolute value of the remainder of the energy flux at different values of  $v$  versus PN order in a log-linear plot. We present results obtained when summing multipoles up to  $\ell = 2$  (circles),  $\ell = 3$  (squares),  $\ell = 4$  (diamonds),  $\ell = 5$  (triangles up),  $\ell = 6$  mode (triangles down) and  $\ell = 8$  (stars).

truncating the sum at  $\ell = 2$  (circles),  $\ell = 3$  (squares),  $\ell = 4$  (diamonds),  $\ell = 5$  (triangles up),  $\ell = 6$  (triangles down) and  $\ell = 8$  (star). Observe that for small velocities (i. e.  $v = 0.01$  or  $v = 0.1$ ) the remainder generally decreases with PN order when using up to  $\ell = 8$  harmonics. This is precisely the convergent-like behavior alluded to earlier. Also observe that an increasing number of multipole moments must be included as a function of PN order to perform any type of meaningful comparison between PN theory and numerical results. We shall study how this number of multipoles depends on velocity in Sec. V.

#### IV. REGION OF VALIDITY

Before applying asymptotic techniques to determine the region of validity, let us show how a quick but *incorrect* estimate can be made directly through Fig. 6. Let us then forget for the moment that higher-order approxima-

tions should be more accurate than lower-order ones, and simply draw a horizontal line in Fig. 6 at some maximum error threshold, such as  $\delta_{\max} = 0.001$ . The required accuracy, of course, depends on the application one has in mind. One can then guarantee that inside some region  $v < \tilde{v}$  the error in the  $N$ th-order PN expansion is less than  $\delta_{\max}$ .

$N$	2	3	4	5	6	7	8	9	10	11
$\tilde{v}$	0.04	0.11	0.14	0.14	0.19	0.30	0.22	0.25	0.28	0.29
$\delta F^{(N)}$ [%]	0.10	0.10	0.10	0.10	0.11	0.11	0.11	0.11	0.11	0.11

TABLE III: For  $v < \tilde{v}$  (second row) the error of using the  $N$ th order PN expansion (where  $N$  is listed in the first row) is less than 0.001, i. e. the relative fractional error  $\delta F^{(N)} \approx 0.1\%$  (second row).

We present  $\tilde{v}$  in Table III, together with the relative fractional error in the energy flux,  $\delta F^{(N)} = (F - F^{(N)})/F$ . This table shows, as expected, that the fractional relative error in the flux is approximately always of the same order, 0.1%. This scheme, however, forces the 11th-order PN approximant to be as accurate as the 2nd-order PN approximant, which is clearly inconsistent with perturbation theory.

The restriction that higher-order approximations be more accurate than lower-order ones is naturally incorporated in the asymptotic estimates of the region of validity, which we shall perform next. The condition defining the edge of the region of validity is

$$\mathcal{O}(F - F^{(N)}) = \mathcal{O}(F^{(N+1)} - F^{(N)}). \quad (19)$$

In other words, we have to determine the  $\tilde{v}$  for which the remainder ceases to be comparable to the next order term.

The remainder and the next-order term possess two distinct and generic features when compared to each other. Figure 8 presents the  $n = 2$  ( $n = 6$ ) order remainders, as well as the  $n = 3$  ( $n = 7$ ) order term in the top (bottom) panel as a function of velocity. The two distinct behaviors alluded to earlier are the following: either the remainder and the next-order term are of the same order for sufficiently low velocities, until eventually the curves separate for larger velocities; or the next-order term starts off smaller than the remainder, but eventually the curves cross and separate. When the curves

cross (in the bottom panel, this crossing occurs roughly at  $v \approx 0.275$ ) one can apply the same techniques of the previous section and simply define  $\tilde{v}$  as the velocity where the curves intersect. However, when the curves do not cross (top panel), we must extend the methods we used for Bessel functions.

The asymptotic analysis definition of the edge of the region of validity is inherently ambiguous, depending on the precise meaning of the order symbol. Let us then

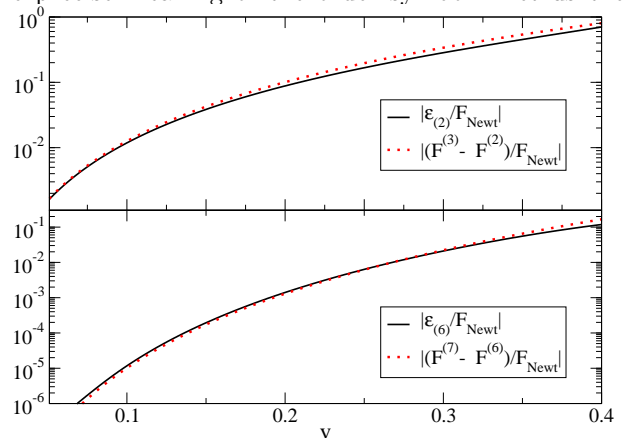


FIG. 8: Top: Log-linear plot of the absolute value of the remainder of the  $N = 2$  PN flux in the extreme-mass ratio limit (solid) and the  $N = 3$  term (dotted). Bottom: Same as top, but for the  $N = 6$  remainder and the  $N = 7$  term. All curves have been factored by the leading-order, Newtonian expression for the energy flux.

replace Eq. (19) by

$$\left| F - F^{(N)} \right| - \left| F^{(N+1)} - F^{(N)} \right| < \delta, \quad (20)$$

where  $\delta$  is some tolerance. One would expect this tolerance to decrease with PN order, since higher-order approximations should be more sensitive to smaller differences. Let us, however, forget this for the moment and demand a *constant* tolerance  $\delta = 10^{-3}$ . This procedure is somewhat similar to picking a maximum error threshold in the remainders of the approximation, which we already explored in Table III. Here, however, we do not demand a constant maximum error, but instead we arbitrarily choose a constant *relative difference* between the remainder and the next term in the series.

$N$	2	3	4	5	6	7	8	9	10
$\tilde{v}(\delta\tilde{v})$	0.107(0.017)	0.138(0.021)	0.140(0.017)	0.190(0.020)	0.266(0.045)	0.222(0.019)	0.248(0.019)	0.281(0.018)	0.292(0.019)
$\delta F$ [%]	1.51	0.29	0.11	0.61	1.03	0.02	0.28	0.35	0.16

TABLE IV: Approximate values of the edge of the region of validity for different orders of the EMRI-PN energy flux. The first row lists  $\tilde{v}$  and (in parentheses)  $\delta\tilde{v}$ ; the second row lists  $\delta F^{(N)} = (F - F^{(N)})/F$ , evaluated at  $\tilde{v}$ .

Applying this procedure, one obtains the  $\bar{v}$  and its error  $\delta\bar{v}$  presented in Table IV. Here  $\delta\bar{v}$  symbolizes variations of the tolerance in the interval  $\delta = \{10^{-3}/5, 5 \times 10^{-3}\}$ , i. e. we evaluate  $\bar{v}_1$  ( $\bar{v}_2$ ) with  $\delta_1 = 10^{-3}/5$  ( $\delta_2 = 5 \times 10^{-3}$ ) and define the error as  $\delta\bar{v} := |\bar{v}_1 - \bar{v}_2|/2$ . As one can see from Table IV, the relative fractional error decreases on average with PN order, although not monotonically.

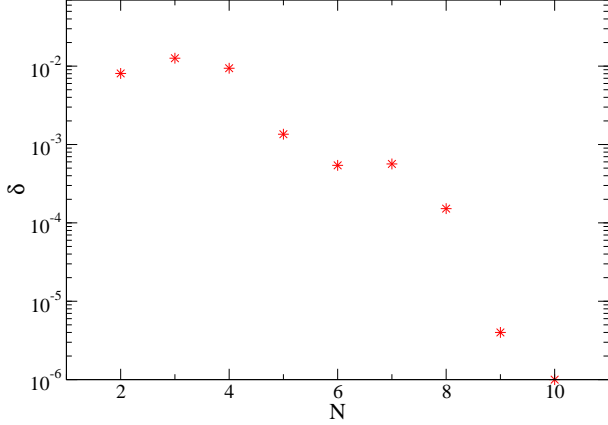


FIG. 9: Tolerance as a function of PN order.

Higher-order approximations should be sensitive to a smaller tolerance, which implies that this quantity can-

not be set arbitrarily. Instead,  $\delta$  should be given by the error in the difference between the  $N$ th remainder and the  $(N + 1)$ th-order term. This error is presumably of the order of the error in the  $(N + 1)$ th-order term, and it can be estimated by the  $(N + 2)$ th-order term. This quantity, of course, depends on  $v$ , but its order can be roughly given by its absolute value evaluated in the middle of its range  $v \approx 0.2$ . By this method we estimate that the tolerance behaves with PN order as shown in Fig. 9. Since this estimate of the tolerance is not exact, we shall allow  $\delta$  to vary between 5 times and 1/5 times its value. In this way, we can determine the sensitivity of our results to the choice of  $\delta$  and provide error bars as done previously.

The edge of the region of validity can now be computed using the tolerance criterion defined above. Table V presents  $\bar{v}$ , together with an averaged error bar  $\delta\bar{v}$ , which represents variations of  $\{\delta/5.0, 5.0 \delta\}$ . The first line in the first row of this table uses the tolerance presented in Fig. 9. Observe that the relative fractional error in the flux, the first line in the second row of Table V, decreases on average as the order of the approximation increases. However, the region of validity seems to increase between 2nd and 6th PN order (except as one goes from 4 to 5), while it seems to decrease between 6th and 10th PN order. We shall analyze this behavior in more detail shortly.

$N$	2	3	4	5	6	7	8	9	10
$\bar{v}(\delta\bar{v})$	0.179(0.029)	0.200(0.014)	0.207(0.025)	0.199(0.021)	0.288(0.007)	0.207(0.018)	0.204(0.016)	0.178(0.010)	0.160(0.006)
	0.160(0.026)	0.200(0.014)	0.214(0.026)	0.197(0.021)	0.346(0.019)	0.214(0.018)	0.207(0.016)	0.158(0.005)	0.179(0.029)
	0.143(0.023)	0.200(0.014)	0.221(0.027)	0.195(0.020)	0.390(0.024)	0.222(0.019)	0.211(0.016)	0.160(0.101)	0.160(0.101)
$\delta F$ [%]	6.7607	-1.3250	-0.5562	0.7888	-1.6931	-0.0134	0.0518	-0.0043	0.0001
	4.8505	-1.3250	-0.6269	0.7531	-5.2159	-0.0151	0.0592	-0.0014	0.0005
	3.5011	-1.3250	-0.7065	0.7103	-9.6392	-0.0168	0.0686	-0.0015	0.0001

TABLE V: First row: edge of the region of validity  $\bar{v}$  and (in parentheses) estimated error  $\delta\bar{v}$ . Second row:  $\delta F^{(N)}$  [%] with the tolerance set by the  $(N + 2)$ th-order term in the approximation. Top to bottom, we list values corresponding to three successive iterations of our attempt to estimate the region of validity (see text).

Before discussing the implications of these results, let us attempt to determine how reliable they are by experimenting with the choice of  $\delta$ . Let us then continue to define the tolerance through the  $(N + 2)$ th-order term, but this time let us evaluate it at the value of  $\bar{v}$  found in the first line of the first row of Table V. Doing so, we obtain the values of  $\bar{v}$  presented in the second line of the

first row of this table. If we iterate this algorithm once more and use the second line in the first row of Table V to evaluate the  $(N + 2)$ th-order term, we obtain yet another  $\bar{v}$ , given in the third line of the first row of this table.

The edge of the region of validity seems to be rather insensitive to the choice of  $\delta$ , provided the  $(N + 2)$ th-order term is not evaluated too far from the mean of the

domain. Indeed, Table V shows that for most values of  $N$  the value of  $\bar{v}$  given in the first row remains within the error bars of the first line of the first row. This is not the case for  $N = (9, 10)$ , because then the values of  $\delta F$  obtained are at the level of the numerical accuracy of our simulations:  $\delta F^{(9,10)} \approx 10^{-6}$ . This is also not the case for  $N = 6$ , because this is an inflection point in the behavior of the edge of the region of validity, and thus the first iteration forces  $\bar{v}$  outside of this region. We therefore conclude that the first line in the first row of Table V suffices as a reliable, approximate measure of the edge of the region of validity of the PN approximation.

A note of warning is due at this point: the iterative scheme presented here should not be confused with a convergence scheme. One might be tempted to expect that as we continue to iterate,  $\bar{v}$  will tend to some definite value that will unequivocally define the region of validity exactly. This concept, however, is inherently flawed because asymptotic series by definition do not possess an exact region of validity. As already explained, asymptotic series and their region of validity are defined via order symbols, and thus can only be interpreted as approximate concepts.

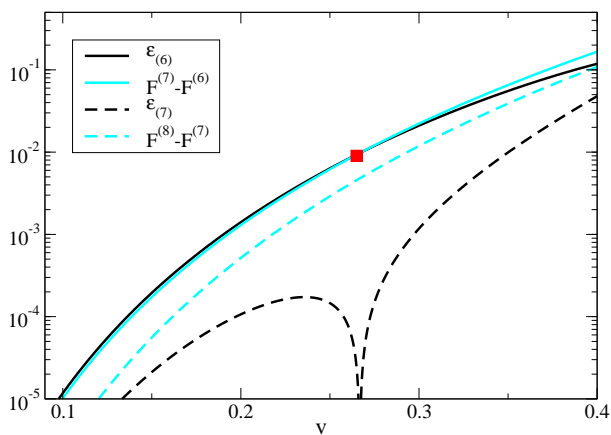


FIG. 10: Plot of  $\epsilon_{(6)}$  (solid black),  $\epsilon_{(7)}$  (dashed black), the 7th-order term (solid light gray) and the 8th-order term (dashed light gray). The square shows where  $\epsilon_{(6)}$  and  $(F^{(7)} - F^{(6)})$  cross.

Let us now discuss the behavior of the edge of the region of validity with PN order in more detail. As we already mentioned, there seems to be an inflection point at  $N = 6$ : on average,  $\bar{v}$  increases for  $N < 6$ , while it decreases for  $N > 6$ . Such a behavior then forces the  $N = 6$  approximation to have the largest region of validity. By naively inspecting Fig. 6 one could be tempted to conclude that this result is paradoxical, since  $\epsilon_{(7)} < \epsilon_{(6,8)}$ . However, recall that the region of validity is determined by the difference between  $\epsilon_{(N)}$  and the  $(N + 1)$ th-order term (*not*  $\epsilon_{(N+1)}$ ). To stress this difference, in Fig. 10 we show  $\epsilon_{(6)}$ ,  $\epsilon_{(7)}$  (black) and the 7th- and 8th-order terms (light gray). Although the absolute value of  $\epsilon_{(7)}$  is smaller than  $\epsilon_{(6)}$ , observe that  $\epsilon_{(6)} \approx F^{(7)} - F^{(6)}$  in a large ve-

locity range, until the curves cross around  $\bar{v} = 0.265$ . On the other hand,  $\epsilon_{(7)} \approx F^{(8)} - F^{(7)}$  only for  $v < 0.2$ , and soon after the curves separate. We see then that the absolute magnitude of the remainder itself does not determine the region of validity. As we stress once more, this region is defined by the requirement that the error in the approximation is smaller than (or of the same order as) the next-order term in the series.

The behavior of the edge of the region of validity with PN order was already presented in the Introduction (Fig. 1). Whether there is truly a negative slope for  $N > 9$  is difficult to establish due to the truncation error, but our results seem to support this hypothesis. Nonetheless, we do observe in the figure that for  $N < 6$  the region of validity increases (as expected of a convergent series), while for  $N > 6$  it decreases (as expected of a divergent series). Such a result seems to agree with the statement that the logarithmic terms in the PN approximation somewhat destroy the convergence properties of the series [8–10]. Nonetheless, as we have seen in this paper, a divergent series can sometimes be even more useful and accurate than a convergent one, provided it is used within its region of validity.

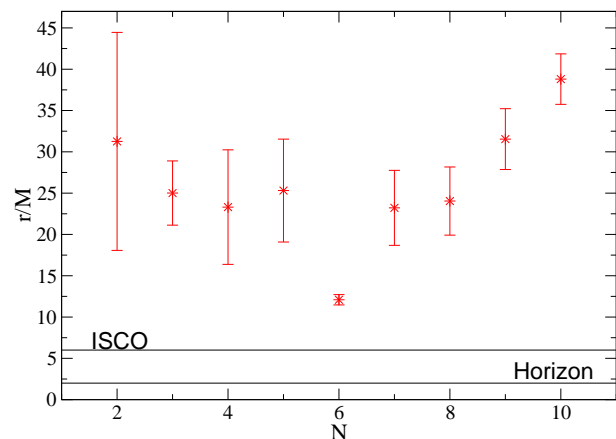


FIG. 11: Minimum orbital radius [Eq. (21)] representation of the edge of the region of validity for different PN orders.

The edge of the region of validity can also be presented as a function of the Schwarzschild radius of the particle's circular orbit. Figure 11 shows the minimum Schwarzschild radius delimiting the region of validity, as a function of PN order. This radius can be obtained from  $\bar{v}$  through the generalization of Kepler's law to circular geodesics:

$$\frac{r}{M} = \frac{1}{v^2}. \quad (21)$$

Simone *et al.* determined that the PN approximation for the infall of a particle into a Schwarzschild black hole can be trusted down to a harmonic radius  $r_{\text{harm}} \simeq 10M$  [11]. Perhaps it is no coincidence that their final result is surprisingly close to the edge of the region of validity for the 3PN approximant of the flux for quasi-circular inspirals.

The results presented so far should not be misinterpreted as saying, for example, that the 3PN approximation is more accurate than higher-order ones. In fact, the statements made here say nothing about the absolute accuracy of the PN approximation. These results only suggest relational statements between the  $N$ th and the  $(N + 1)$ th-order approximations. Table V should be read as saying that, for velocities  $v < \bar{v}$ , the  $N$ th order approximation has errors that are of expected relative size. For larger velocities, the  $(N+1)$ th- and higher-order terms become important, and should not be formally neglected. However, if one is willing to tolerate errors larger than those estimated by the  $(N + 1)$ th order term, and if one is willing to relinquish the desire that higher-order approximation be more accurate than lower-order ones, then one can surely go beyond  $\bar{v}$  at the cost of losing analytic control of the magnitude of the error.

## V. MULTIPOLES AND PN ORDERS

As a by-product of this analysis, we can ask the following interesting question: how many multipoles should be kept in the numerical solution if we are interested in studying the  $N$ th-order PN approximation? In other words, we wish to determine whether it is sufficient to keep only the quadrupole in certain cases, or if we always need higher multipoles to study the accuracy of the PN series (see [34] for a related discussion).

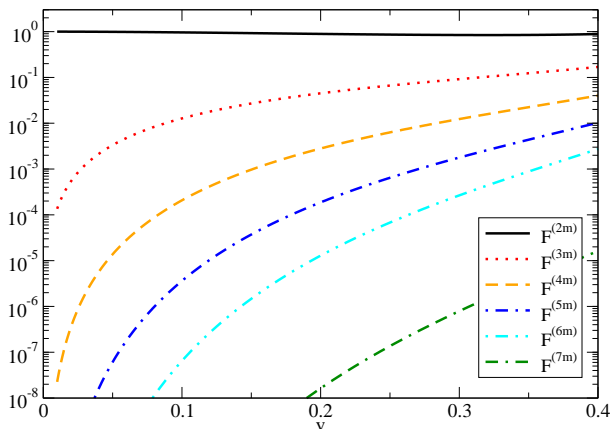


FIG. 12: Plot of the energy flux decomposed into spherical harmonics and summed over  $m$ . Each multipolar component is normalized to the Newtonian flux. The  $\ell = 2$  harmonic is shown with a solid line, the  $\ell = 3$  with a dotted line, the  $\ell = 4$  with a dashed line, the  $\ell = 5$  with a dot-dashed line, the  $\ell = 6$  with a dash-dot-dot line, and the  $\ell = 7$  with a dash-dash-dotted line.

The answer to this question depends on the behavior of each multipolar contribution to the energy flux as a function of velocity. In Fig. 12 we plot multipolar contributions with different  $\ell$ 's (where for each  $\ell$  we sum over all values of  $m$ ) normalized to the Newtonian flux. The dominant ( $\ell = 2$ ) mode is very close to unity for all val-

ues of  $v$ , while all other contributions go to zero as  $v \rightarrow 0$  and approach a roughly constant,  $\ell$ -dependent value. We do not show in the figure the  $\ell = 8$  harmonic to avoid cluttering, but this contribution would be located at the lower right corner of the figure.

Figure 12 implies that it is ludicrous to compare PN with numerical relativity in certain systems if only a few multipoles are taken into account. For example, neglecting the  $\ell = 4$  multipole leads to errors of  $\mathcal{O}(10)^{-4}$  at  $v = 0.1$ , which is comparable to terms of  $\mathcal{O}(1/c)^4$ . Thus, comparing PN expansions of  $\mathcal{O}(1/c)^5$  and smaller to numerical solutions neglecting the  $\ell = 4$  multipole at  $v < 0.1$  is risky and may lead to incorrect conclusions. The relative importance of higher- $\ell$  multipoles decreases for equal mass systems, but again recovers great importance when eccentricity and/or spins are included.

The number of multipoles to retain also depends on the PN contribution to the energy flux. Figure 13 plots these contributions, normalized to the Newtonian flux. As be-

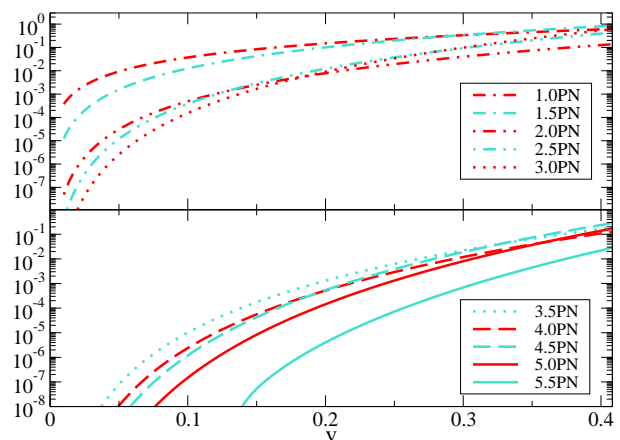


FIG. 13: Plot of the relative PN contributions to the total energy flux normalized to the Newtonian flux. Top: PN orders  $\mathcal{O}(1/c^2)$  to  $\mathcal{O}(1/c^6)$ . Bottom: PN orders  $\mathcal{O}(1/c^7)$  to  $\mathcal{O}(1/c^{11})$ .

fore, odd (even) orders are plotted in light (dark) gray. Observe that the PN contributions of the top panel (lower PN orders) rise rather fast and approach a roughly constant value. The opposite is true for the bottom panel, where the curves are monotonically increasing in this velocity domain.

An analysis of the accuracy of the  $N$ th-order PN approximation requires that the numerical error be at the very least smaller than the  $N$ th-order term. In the asymptotic analysis of the previous section, we simply summed up to  $\ell = 8$  and always included all harmonics in our analysis. However, it is possible that we did not need to keep up to  $\ell = 8$  in the analysis of all PN orders. Figure 14 superimposes the PN contribution and the multipolar contribution of the energy flux. We see, for example, that the  $\ell = 5$  harmonic contribution is always negligible if one is studying a 1.5PN order accurate expression.

The intersection of the harmonic and PN contribu-

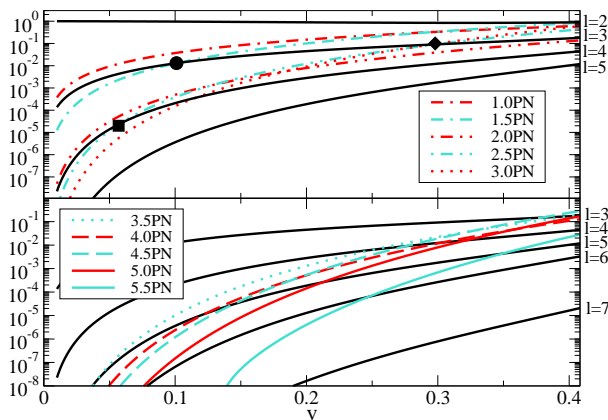


FIG. 14: Same as Figs. 12 and 13. The black solid curves are the harmonic contributions to the energy flux, while the non-solid curves represent the PN contributions. The intersections in this figure (some of which are shown as a square, a diamond or a circle) lead to Table I in the Introduction.

tions provide a *minimum* requirement of accuracy if any type of comparison between numerical simulations and PN theory is to be carried out. These intersections form the basis of Table I in the Introduction. For example, if one wishes to compare numerical results to the 1.5PN energy flux, then one can simply use the  $\ell = 2$  harmonic provided  $v > 0.101$  (shown as a circle in the figure). For smaller velocities, however, the  $\ell = 3$  harmonic contribution needs to be included. Similarly, if one is studying the 2.5PN expression of the energy flux, then one can simply use the  $\ell = 2$  harmonic if  $v > 0.298$  (shown as a diamond in the figure), but one must include the  $\ell = 3$  harmonic if  $0.057 < v < 0.298$  and the  $\ell = 4$  harmonic if  $v < 0.057$  (a square in the figure). Finally, note that the number of multipoles that need to be included is larger for smaller velocities. This is because the multipolar contribution raises steeply for small velocities and then roughly asymptotes to a constant, leading to more intersections when  $v$  is small.

## VI. CONCLUSIONS AND OUTLOOK

We have proposed a generic, gauge-independent and systematic method to determine the formal region of validity of the PN approximation. This method relies heavily on tools from asymptotic analysis, and in particular, on the concept of an optimal asymptotic expansion. The main philosophy of the approach is to determine the velocity or frequency beyond which the next-order term in the series must be included. This velocity is found by studying the region where the true error in the approximation (relative to the exact or numerical answer) becomes comparable to the series truncation error (due to neglecting higher-order terms in the series).

We applied this method to the quasi-circular inspiral of a small compact object into a non-spinning black hole.

The PN approximation is thus coupled to an EMR expansion, leading to what we here called the PN-EMR approximation. The exact solution is modeled by a numerical calculation in black hole perturbation theory. This scheme linearizes the Einstein equations in the metric perturbation but not in the velocity parameter, and so it is suitable for the study of EMR systems. Here we are mainly interested in a proof-of-principle of the proposed method and we used the energy flux as the dependent variable, but we could have studied other time-dependent quantities. The gravitational wave phase, for example, is the most interesting quantity for data analysis purposes. However, relating the energy flux to the phasing involves a certain degree of arbitrariness (see [35] for a discussion) and we preferred to avoid these complications in our preliminary exploration.

The output of the method is the edge of the region of validity as a function of PN order (Fig. 1). We found that the 3PN approximation of the energy flux seems to possess the largest region of validity. This implies that the 3PN approximation can be evaluated up to rather high velocities (i. e.  $v \approx 0.29$ ) and still produce an approximate answer with an error of expected size (given by the next order term in the series). Moreover, we found that for lower than 3PN order, the PN approximation seems to present a convergent-like behavior (the region of validity increases with PN order). Similarly, PN approximants of order higher than 3PN present a divergent-like behavior (the region of validity decreases with PN order), probably associated with the appearance of logarithmic terms in the series.

Another result of this paper is the *minimum* number of multipoles that need to be retained to perform any type of comparison with PN theory (Table I). We find that the number of multipoles depends on the velocity regime where the comparison takes place. In particular, we find that more multipoles are required for low velocities. At 3.5PN order, the inclusion of the first five multipoles suffices to cover the entire velocity range. It will be interesting to explore the number of multipolar components that must be included in a numerical simulation of comparable mass binaries to get some required accuracy in the *phasing* of the waves.

Although the method is generic and gauge-independent, the conclusions derived from the analysis of EMR systems are not necessarily generalizable to comparable mass systems. The number of multipoles needed to match the flux in the comparable mass case is probably smaller than suggested here. Moreover, the PN series is suspected to be much less accurate for EMR systems, which suggests that perhaps for comparable mass systems the onset of the divergent-like behavior observed here could occur at higher PN orders.

Various extensions of this work should be possible in the near future. In particular, we would like to consider:

- 1) Other physical systems: Although we have here studied only non-spinning EMR systems, the proposed method is very general and it can be applied

to more complex physical scenarios. For example, by modeling a small particle in orbit around a spinning (Kerr) black hole, one could study whether the black hole's angular momentum substantially affects the region of validity of PN theory. Other interesting scenarios would be comparable-mass, eccentric and spinning binaries. These systems, however, are much more difficult to model, both numerically and in PN theory. In particular, an accurate estimate of numerical errors in present numerical relativistic simulations is quite challenging [35–37].

- 2) Different observables: We have here considered only the energy flux, because it is a well-defined, time-dependent observable. We could, however, also apply this method to the phasing of gravitational waves or the linear and angular momentum fluxes. One expects the asymptotic properties of PN theory to be independent of the quantity analyzed to determine it. If this were the case, the regions of validity found by analyzing, for example, the momentum flux or the phasing should be comparable to those found here. Although unlikely, if this were not the case, then different PN-expanded quantities of the *same* order would possess different regions of validity, casting doubts on the asymptotic structure and consistency of the PN approximation.
- 3) Different PN flavors: The method considered here does not depend on the PN approximant we use. We would like to study the region of validity of other (non-Taylor) PN approximants, such as the effective-one-body approach [5, 6], Padé [3, 4] and Chebyshev resummations [8–10]. In the EMR case, a fully convergent expansion of the flux might in principle be obtained via the Mano-Takasugi method [38–41]. To our knowledge, however, the adiabatic energy flux has not been worked out explicitly in this approach, and their method does not seem to be straightforwardly generalizable to comparable masses.

The studies suggested above would answer a number of questions and shed light on the structure of the PN series. Point (1) would reveal how the region of validity depends on the initial properties of the system. Based on previous studies [18, 19], one would expect this region to increase as the mass ratio approaches unity. Moreover, point (1) would shed light on the possible overlap of different approximation schemes, such as PN theory, black hole perturbation theory and the close-limit approximation [42], providing support to asymptotically matched global solutions [43–45]. Point (3) would allow us to make relative statements about the regions of validity of different PN flavors. One could then verify whether different resummation techniques truly increase the region of validity of the PN approximation (see e. g. [18] for criticism of this idea). In any case, a detailed study of the analytic structure of the PN approximation should greatly

benefit our understanding of the dynamics of inspiraling compact binaries.

### Acknowledgments

We are grateful to Abhay Ashtekar, Carl Bender, Luc Blanchet, Alessandra Buonanno, Vitor Cardoso, Curt Cutler, José González, Yasushi Mino, Ben Owen, Eric Poisson, Uli Sperhake and Clifford Will for useful comments and discussions. N.Y. acknowledges support from National Science Foundation award PHY 05-55628 and the support from the Center for Gravitational Wave Physics, which is funded by the National Science Foundation under Cooperative Agreement PHY 01-14375. E.B.'s research was supported by an appointment to the NASA Postdoctoral Program at the Jet Propulsion Laboratory, California Institute of Technology, administered by Oak Ridge Associated Universities through a contract with NASA. Copyright 2008 California Institute of Technology. Government sponsorship acknowledged.

## Appendix: Logarithmic terms

The presence of logarithmic terms in the PN expansion [see e. g. Eq. (17)] seems inherent to the PN approximation in harmonic coordinates. The question we wish to answer is whether these terms affect the use of standard asymptotic techniques. The answer to this question is in the negative, and we explain why below.

First, Arun et al. [46] have argued that the logarithmic terms can be removed by a coordinate transformation for eccentric comparable-mass binaries. The new, so-called modified harmonic coordinates differ from standard harmonic coordinates to 1PN order and are regular everywhere. Therefore, since the convergence or divergence properties of the approximation should not depend on the coordinate system used, it should not matter whether we do the analysis in harmonic or modified harmonic coordinates. In other words, if we were to repeat the analysis in modified harmonic coordinates, we should arrive at similar conclusions as those found here.

Second, we can re-write the logarithmic terms in the PN approximation in a manner which clearly exhibits its asymptotic structure. Let us define  $\nu \equiv \ln v$ , such that  $\nu \in [-\infty, 0]$  as  $v \in [0, 1]$ . Then we can write

$$\sum_{p=6}^{\infty} a_p v \ln(v^p) = e^{\nu} \sum_{p=6}^{\infty} b_p \nu, \quad (22)$$

where we have absorbed a factor of  $e^p$  into  $b_p$ . We then see that in the new variables this series is reminiscent of a standard asymptotic expansion with an exponential controlling factor (see e. g. [20]).

Third, we can straightforwardly show that the series is indeed asymptotic in some small velocity region. Let us first note that any series  $w_0 = \sum_n a_n v^n$  is indeed an asymptotic series for small  $v$ , which is simply a re-statement that any Taylor expansion is an asymptotic series [20]. Similarly, it follows that a series of the form  $w_1 = \sum_n b_n \ln(v)$  is *not* an asymptotic series, because  $\ln(v)$  diverges as  $v \rightarrow 0$ . Fortunately, the PN expansion does not contain isolated logarithmic contributions. All logarithmic terms are multiplied by some power of the velocity, i. e. the expansion has the form  $w_2 = \sum_n b_n v^n \ln(v)$ . As  $v \rightarrow 0$ , such a series indeed tends to zero and is well-behaved.

Not only should the series be well-behaved as  $v \rightarrow 0$ , but it should also decay at the right rate, i. e. in such a way so that Eq. (5) holds. Let us then look at the  $N = 6$  term in the PN expansion of the energy flux. Since we know that  $a_6 v^6$  decays at the right rate, we can compare  $b_6 v^6 \ln(v)$  to this quantity. One can easily verify that  $a_6 v^6$  is larger than the logarithmic term for  $v \gtrsim 0.033$ , while the opposite is true for smaller velocities. When  $v \approx 10^{-4}$  and smaller, the logarithmic term dominates over the polynomial term, but such small velocities are excluded from our analysis anyway, since we only compute the numerical flux down to  $v = 10^{-2}$ . Therefore the  $N = 6$  term in the PN expansion of the energy flux is

not only well-behaved as  $v \rightarrow 0$ , but it indeed decays at the right rate in the velocity region considered here.

Based on these arguments, we conclude that there exists a small-velocity *near zone* region, where logarithmic terms in the PN series do not affect the asymptotic analysis described in this paper.

## Erratum

This erratum corrects some mistakes in Ref. [47].

By comparison with high-accuracy numerical data produced with an independent code by Scott Hughes, we found out that our numerical solution of the Teukolsky equation (i.e., the numerical data used to approximate the exact solution to the flux function) is only accurate up to  $\ell = 6$ . This implies that the line labeled  $F^{(7m)}$  in Fig. 12 of [47] is in error. For the same reason the data marked by asterisks in Fig. 7 are not accurate, and should be ignored. Note also that the  $x$ -axis in Fig. 7 should range from  $N = 2$  to  $N = 11$ : there is no PN correction to the flux when  $N = 1$ .

More importantly, we found two mistakes in the code that computes the optimal velocity of expansion (the edge of the region of validity). Fortunately, these mistakes do not affect the main conclusion of [47]: that the edge of the region of validity shrinks for  $N > 6$ . Below we discuss these mistakes and correct them, providing updated tables and figures.

The first mistake affects the  $N = 3$  and  $N = 6$  data points. In Fig. 1 and Table V of [47], the edge of the region of validity was found to be  $\bar{v} = 0.2$  and  $\bar{v} = 0.29$  for the  $N = 3$  and  $N = 6$  cases, respectively. These values were obtained through Eq. (20) in [47]:

$$\delta_N(v) \equiv \left| |F - F^{(N)}| - |F^{(N+1)} - F^{(N)}| \right| < \delta. \quad (23)$$

We will refer to this equation as the  $\delta_N$  criterion. Upon more detailed analysis, we have found that in these cases  $\delta_N(v)$  presents zero crossing, so  $N = 3$  and  $N = 6$  correspond to the first class of cases discussed after Fig. 8 in [47]. When such zero-crossings are present, they should be used to define the edge of the region of validity, instead of the  $\delta_N$  criterion. The correct edges of the region of validity are  $\bar{v} = 0.38$  and  $\bar{v} = 0.27$  for the  $N = 3$  and  $N = 6$  cases, respectively.

The second mistake affects the size of the error bars. In [47], these were said to be given by solving Eq. (20) with  $\delta \rightarrow \delta/5$  and  $\delta \rightarrow 5\delta$ . This was a typo in the text: our code solved Eq. (20) with  $\delta \rightarrow \delta/2$  and  $\delta \rightarrow 2\delta$  instead, yielding smaller error bars.

Moreover, for the  $N = 3$  and  $N = 6$  cases, the  $\delta_N$  criterion to define error bars cannot be applied. Instead, one can compute the error as the difference between  $\bar{v}$  and the velocity at which  $|F - F^{(N)}| = |F^{(N+2)} - F^{(N+1)}|$ . Doing so, however, would yield a very large error bar ( $\delta\bar{v} \approx 0.18$ ) for the  $N = 3$  case. Alternatively, in these cases we can compute the error as the difference between



$\bar{v}$  and the *local maxima* in  $\delta_N(v)$ . This is the approach we take here, and it will be justified in more detail in a follow-up paper. Tables VI and VII are a corrected version of Tables IV and V in [47]. They assume a constant  $\delta = 10^{-3}$  and the  $\delta_N$  values in Fig. 9 of [47], respectively.

The error bars quoted for the  $N = 3$  and  $N = 6$  cases correspond to the “local maxima” criterion described above. The primary change in these plots is in the error bars and in the values of  $\bar{v}$  for  $N = 3$  and  $N = 6$ .

$N$	2	3	4	5	6	7	8	9	10
$\bar{v}(\delta\bar{v})$	0.11(0.04)	0.14(0.05)	0.14(0.04)	0.19(0.04)	0.30(0.03)	0.22(0.04)	0.25(0.04)	0.28(0.04)	0.29(0.04)
$\delta F[\%]$	1.5	-0.30	-0.1	0.61	-2.1	-0.02	0.28	-0.35	0.16

TABLE VI: Approximate values of the edge of the region of validity for different orders of the PN energy flux in the extreme mass-ratio limit. The first row lists  $\bar{v}$  and (in parentheses)  $\delta\bar{v}$ ; the second row lists  $\delta F^{(N)} = (F - F^{(N)})/F$ , evaluated at  $\bar{v}$ .

$N$	2	3	4	5	6	7	8	9	10
$\bar{v}(\delta\bar{v})$	0.18(0.08)	0.38(0.06)	0.21(0.06)	0.20(0.05)	0.27(0.03)	0.21(0.04)	0.20(0.03)	0.18(0.02)	0.16(0.01)
	0.16(0.07)	.	0.21(0.06)	0.20(0.05)	.	0.21(0.04)	0.21(0.03)	0.16(0.01)	0.17(0.04)
	0.14(0.06)	.	0.22(0.06)	0.19(0.05)	.	0.22(0.04)	0.21(0.03)	0.15(0.01)	0.15(0.01)
$\delta F[\%]$	6.8	-9.5	-0.56	0.79	-1.0	-0.013	0.052	-0.0043	0.0001
	4.8	.	-0.63	0.74	.	-0.016	0.060	-0.0014	0.00002
	3.5	.	-0.71	0.7	.	-0.017	0.070	-0.0007	0.00002

TABLE VII: First row: edge of the region of validity  $\bar{v}$  and (in parentheses) estimated error  $\delta\bar{v}$ . Second row:  $\delta F^{(N)}$  [%] with the tolerance set by the  $(N + 2)$ th-order term in the approximation. Top to bottom, we list values corresponding to three successive iterations of our attempt to estimate the region of validity (see text). Error bars for the  $N = 3$  and  $N = 6$  terms are given by the local maxima criteria.

The graphical representation of these tables must also be corrected. The correct version of Figs. (1) and (11) of [47] is Fig. 15 of this Erratum. Observe that the error bars have become larger. Moreover, notice that for  $N = 3$  and  $N = 6$   $\bar{v}$  is now much larger than for other values of  $N$  (and the opposite happens for  $b$ ). This is again because of the zero-crossing behavior of these special points. More details will be given in an upcoming

publication [48]. We reiterate, however, that although the  $N = 3$  and  $N = 6$  points have changed, and the error bars have become larger, the main conclusion of [47] (that the edge of the region of validity shrinks for  $N > 6$ ) still holds.

Finally, note that Eq. (18) of [47] contains a typo:  $M^2$  should be replaced by  $M^{-2}$ .

[1] F. Pretorius (2007), arXiv:0710.1338 [gr-qc].  
[2] C. Cutler et al., Phys. Rev. Lett. **70**, 2984 (1993), astro-ph/9208005.  
[3] T. Damour, B. R. Iyer, and B. S. Sathyaprakash, Phys. Rev. **D57**, 885 (1998), gr-qc/9708034.  
[4] T. Damour, B. R. Iyer, and B. S. Sathyaprakash, Phys. Rev. **D62**, 084036 (2000), gr-qc/0001023.  
[5] A. Buonanno and T. Damour, Phys. Rev. **D59**, 084006 (1999), gr-qc/9811091.  
[6] A. Buonanno and T. Damour, Phys. Rev. **D62**, 064015 (2000), gr-qc/0001013.

[7] T. Damour and A. Nagar (2007), arXiv:0711.2628 [gr-qc].  
[8] E. K. Porter (2005), gr-qc/0510121.  
[9] E. K. Porter, Class. Quant. Grav. **23**, S837 (2006), gr-qc/0609015.  
[10] E. K. Porter, Phys. Rev. **D76**, 104002 (2007), arXiv:0706.0114 [gr-qc].  
[11] L. E. Simone, E. Poisson, and C. M. Will, Phys. Rev. **D52**, 4481 (1995), gr-qc/9506080.  
[12] L. E. Simone, S. W. Leonard, E. Poisson, and C. M. Will, Class. Quant. Grav. **14**, 237 (1997), gr-qc/9610058.  
[13] E. Poisson, Phys. Rev. **D47**, 1497 (1993).

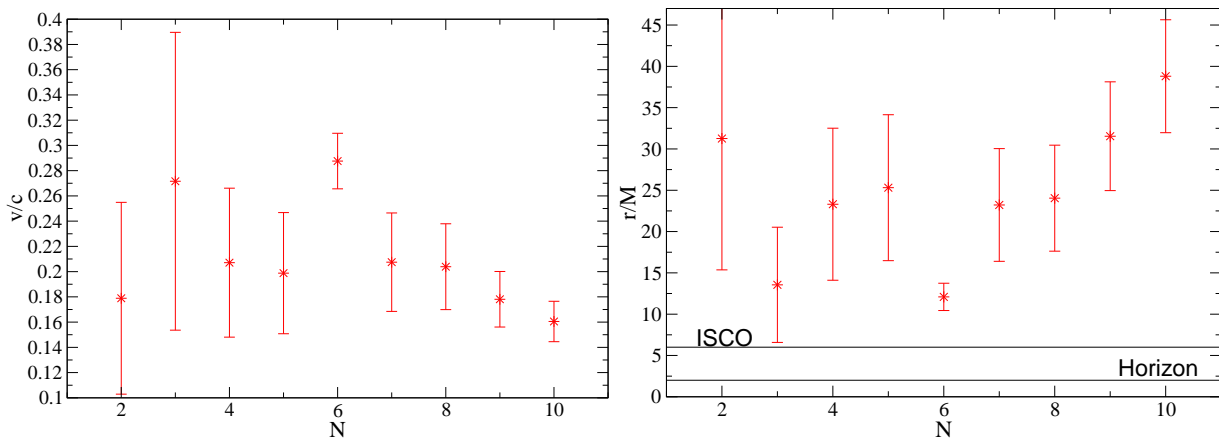


FIG. 15: Left: Edge of the region of validity for different PN orders. Right: Minimum orbital radius representation of the edge of the region of validity for different PN orders. Error bars for the  $N = 3$  and  $N = 6$  terms are given by the local maxima criteria.

- [14] E. Poisson and M. Sasaki, Phys. Rev. **D51**, 5753 (1995), gr-qc/9412027.
- [15] H. Tagoshi and M. Sasaki, Prog. Theor. Phys. **92**, 745 (1994), gr-qc/9405062.
- [16] T. Tanaka, H. Tagoshi, and M. Sasaki, Prog. Theor. Phys. **96**, 1087 (1996), gr-qc/9701050.
- [17] E. Poisson, Phys. Rev. **D52**, 5719 (1995), gr-qc/9505030.
- [18] L. Blanchet (2002), gr-qc/0207037.
- [19] T. Mora and C. M. Will, Phys. Rev. **D69**, 104021 (2004), gr-qc/0312082.
- [20] C. M. Bender and S. A. Orszag, *Advanced mathematical methods for scientists and engineers 1, Asymptotic methods and perturbation theory* (Springer, New York, 1999).
- [21] T. Mora and C. M. Will, Phys. Rev. **D66**, 101501 (2002), gr-qc/0208089.
- [22] E. Berti, S. Iyer, and C. M. Will, Phys. Rev. **D74**, 061503 (2006), gr-qc/0607047.
- [23] E. Berti, S. Iyer, and C. M. Will, Phys. Rev. **D77**, 024019 (2008), arXiv:0709.2589 [gr-qc].
- [24] C. W. Misner, K. Thorne, and J. A. Wheeler, *Gravitation* (W. H. Freeman & Co., San Francisco, 1973).
- [25] J. Kevorkian and J. D. Cole, *Multiple scale and singular perturbation methods* (Springer, New York, 1991), and references therein.
- [26] M. Abramowitz and I. A. Stegun, *Handbook of Mathematical Functions with Formulas, Graphs, and Mathematical Tables* (Dover, New York, 1964).
- [27] C. Cutler, E. Poisson, G. J. Sussman, and L. S. Finn, Phys. Rev. **D47**, 1511 (1993).
- [28] C. Cutler, D. Kennefick, and E. Poisson, Phys. Rev. **D50**, 3816 (1994).
- [29] L. Gualtieri, E. Berti, J. A. Pons, G. Miniutti, and V. Ferrari, Phys. Rev. **D64**, 104007 (2001), gr-qc/0107046.
- [30] J. A. Pons, E. Berti, L. Gualtieri, G. Miniutti, and V. Ferrari, Phys. Rev. **D65**, 104021 (2002), gr-qc/0111104.
- [31] E. Berti, J. A. Pons, G. Miniutti, L. Gualtieri, and V. Ferrari, Phys. Rev. **D66**, 064013 (2002), gr-qc/0208011.
- [32] E. Berti, Ph.D. thesis, Università Degli Studi Di Roma, La Sapienza (2001).
- [33] W. H. Press, B. P. Flannery, S. A. Teukolsky, and W. T. Vetterling, *Numerical Recipes: The Art of Scientific Computing* (Cambridge University Press, Cambridge (UK) and New York, 1992).
- [34] Y. Mino, M. Sasaki, M. Shibata, H. Tagoshi, and T. Tanaka, Prog. Theor. Phys. Suppl. **128**, 1 (1997), gr-qc/9712057.
- [35] M. Boyle et al., Phys. Rev. **D76**, 124038 (2007), arXiv:0710.0158 [gr-qc].
- [36] A. Buonanno, G. B. Cook, and F. Pretorius, Phys. Rev. **D75**, 124018 (2007), gr-qc/0610122.
- [37] E. Berti et al., Phys. Rev. **D76**, 064034 (2007), gr-qc/0703053.
- [38] S. Mano and E. Takasugi, Prog. Theor. Phys. **97**, 213 (1997), gr-qc/9611014.
- [39] S. Mano, H. Suzuki, and E. Takasugi, Prog. Theor. Phys. **96**, 549 (1996), gr-qc/9605057.
- [40] S. Mano, H. Suzuki, and E. Takasugi, Prog. Theor. Phys. **95**, 1079 (1996), gr-qc/9603020.
- [41] R. Fujita and H. Tagoshi, Prog. Theor. Phys. **112**, 415 (2004), gr-qc/0410018.
- [42] R. H. Price and J. Pullin, Phys. Rev. Lett. **72**, 3297 (1994), gr-qc/9402039.
- [43] N. Yunes, W. Tichy, B. J. Owen, and B. Bruegmann (2005), gr-qc/0503011.
- [44] N. Yunes and W. Tichy, Phys. Rev. **D74**, 064013 (2006), gr-qc/0601046.
- [45] N. Yunes, Class. Quant. Grav. **24**, 4313 (2007), gr-qc/0611128.
- [46] K. G. Arun, L. Blanchet, B. R. Iyer, and M. S. S. Quasailah (2007), arXiv:0711.0302v1.
- [47] N. Yunes, E. Berti, Phys. Rev. **D77**, 124006 (2008), [arXiv:0803.1853 [gr-qc]].
- [48] Z. Zhang, N. Yunes, E. Berti, “Accuracy of the post-Newtonian approximation. II. Optimal asymptotic expansion of the energy flux for quasicircular, extreme mass-ratio inspirals into a Kerr black hole,” to appear.